APERTURE SYNTHESIS TELESCOPES: CARMA, ALMA & MILLIMETER WAVE VLBI

M. C. H. Wright
Radio Astronomy laboratory, University of California, Berkeley, CA, 94720

October 9, 2013

OUTLINE OF TALK

- APERTURE SYNTHESIS TELESCOPES
- ANGULAR RESOLUTION
- MILLIMETER WAVE ASTRONOMY
- MILLIMETER WAVE VLBI

RADIO ASTRONOMY

- Radio astronomy is an observational science.
  - We make images of the radio intensity

$$I(\mathbf{s}, \nu, polarization, time)$$

- What we actually measure is

$$I' = I * B + noise$$

  - B is the instrumental response.
  - $noise$ from receivers, telescope, and atmosphere.
- Data reduction: process of obtaining I from our measurements, I'
  - Calibration and Imaging.
- Data Analysis: interpreting what I means for astronomy.

- **Collecting area $\sim D^2$**

  Antennas collect radio photons from astronomical sources.

$$Power = \int I(s)\ A(s)\ \delta\Omega\ \delta\nu\ \delta A$$

  $A(\mathbf{s})$ is antenna collecting area in direction $\mathbf{s}$ in sky.

$$Power = S[watts\ m^{-2}\ \mathrm{Hz}^{-1}] \times \Delta\nu[Hz] \times A[m^2]$$

  e.g. 1 Jy source with 1 GHz bandwidth and 100m telescope

$$P[watts] = 10^{-26}[watts\ m^{-2}\ \mathrm{Hz}^{-1}] \times 10^{9}[Hz] \times 10^{4}[m^2]$$

$$= 10^{-13} watts \sim 10^{-5.5} Joules/year$$

  Heats 1 mg water 1 mK in 1 year !!

- **Resolution** $\sim \lambda/D$

  Antenna Voltage pattern in direction s

$$v(\mathbf{s}) = \int W(\mathbf{r})\ E(\mathbf{r})\ \exp(2\pi i\ \mathbf{r}.\mathbf{s}/\lambda)\ \delta A$$

  weighted vector average of the E-field across the aperture

  Sum the E-field across the aperture in phase.

$$\rightarrow\rightarrow\rightarrow\rightarrow\rightarrow\rightarrow \text{ in direction } s.$$

- Phase gradients across aperture give telescope angular resolution.

- Uniformly weighted square aperture diameter D,

$$v(\mathbf{s}) = \int exp(2\pi i\ x\ sin(\theta)/\lambda)\ dx \quad [x = -D/2, D/2]$$

$$v(\theta) = \sin(\pi\ \theta\ D/\lambda)/(\pi\ \theta\ D/\lambda)$$

- Uniformly weighted circular aperture diameter D,

$$v(\theta) = 2J_1(\pi\ \theta\ D/\lambda)/(\pi\ \theta\ D/\lambda)$$

- Antenna power pattern

$$P(\mathbf{s}) = v(\mathbf{s}) \times v^{\star}(\mathbf{s})$$

- Circular aperture diameter D with Gaussian weighting.

  Primary beamwidth, FWHM $\sim 1.2\ \lambda/D$

APERTURE SYNTHESIS ARRAYS

- Arrays separate the functions of **resolution** and **collecting area**.
- Antenna arrays sample the wavefront across a distributed aperture
  - we measure the coherence of the wavefront across the array.
  - signal transmission from the antennas preserves phase.
  - keep path lengths within $\sim \lambda/20$ to make an accurate telescope
- Atmospheric fluctuations distort the wavefront.
  - we compensate for these effects. This is quite difficult.
- The problem is rather like adaptive optics.

SENSITIVITY AND RESOLUTION

- Array of N antennas, each with diameter D
- Collecting area and point source sensitivity $\sim ND^2$
- Field of view of antennas, FOV $\sim \lambda/D$.
- Mapping extended sources $>$ FOV needs multiple pointings.

  Mosiacing ($N_{pointings} \sim 1/FOV^2$). Sensitivity $\sim ND$
- Spatial Dynamic Range:

  Range of angular scales mapped by array $\sim \lambda/D_{min} - \lambda/D_{max}$

  D_{min} and D_{max} are smallest and largest antenna separations.
- Antenna cost $\sim ND^2\ \lambda^{-0.7}$, where surface accuracy $\sim \lambda/20$

SINGLE DISH RESOLUTION

- Early radio observations mapped the Galaxy.
- Peaks named Cas A, Cygnus A, Sag A, Taurus A, Virgo A etc.

  Resolution ~ 7 degrees.

  Arecibo: $\lambda/D \sim 6cm/300m \sim 36$ arcsec.

  Bonn: $\lambda/D \sim 1cm/100m \sim 20$ arcsec.

  IRAM 30m: $\lambda/D \sim 1.5mm/30m \sim 10$ arcsec.

  Small optical telescope $\lambda/D \sim 5\ 10^{-5}/10\,\mathrm{cm} \sim 1$ arcsec.
- Single aperture telescopes are confusion limited.

  Large antennas have enough sensitivity,

  but not enough resolution to map source structure.

RADIO SOURCE STRUCTURE AND SPATIAL DYNAMIC RANGE

- Small scale structure in radio sources:
  - galactic nuclei, hot spots in radio galaxies $\sim$ 0.1 - 1 arcsec
  - molecular jets, filaments in crab nebula $\sim$ 1 arcsec
  - IR sources, star formation regions $\sim$ 1 - 10 arcsec
  - molecular cloud structure $\sim$ 0.1 arcsec - several degrees
  - spiral arm structure in galaxies $\sim$ 1 arcsec - a few degrees
  - quasars: VLBI $\lambda/D \sim 1.3\,\mathrm{mm}/5000\,\mathrm{km} \sim 50$ micro arcsec.
- Spatial Dynamic Range

  Range of angular scales mapped by telescope.
  - single antennas can image structures larger than $\sim 20''$ at 3mm.
  - need telescope diameter $\sim$ 1 kilometer to see arcsec structures.

SINGLE DISH TELESCOPE

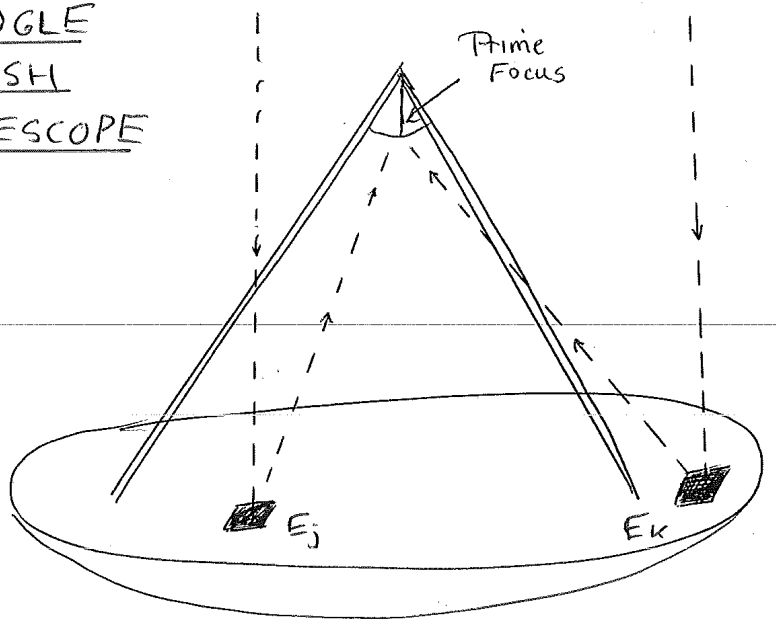

Voltage Response $= \sum_j \underset{\sim}{E}_j$ vector sum of E Field

Power $= \left(\sum_j \underset{\sim}{E}_j\right)\left(\sum_k \underset{\sim}{E}_k\right)^*$

$= \sum_j |E_j|^2 + \sum_j \sum_k E_j E_k^*$

Sum of power + cross products of all pairs

measures coherence of wavefront across telescope

RESPONSE OF SINGLE DISH

SINGLE DISH TELESCOPES

- Voltage response $= \Sigma\ E_j$

  vector sum of E-field across telescope.

- Power $= (\ \Sigma\ E_j)(\Sigma\ E_k)^*$

  $= \Sigma\ E_j^2 + \Sigma\ E_j\ E_k^*$

  = sum of power + cross products of E-field across aperture.

- Cross products measure wavefront coherence across the aperture

  and give the telescope angular resolution.

SINGLE DISH RESOLUTION

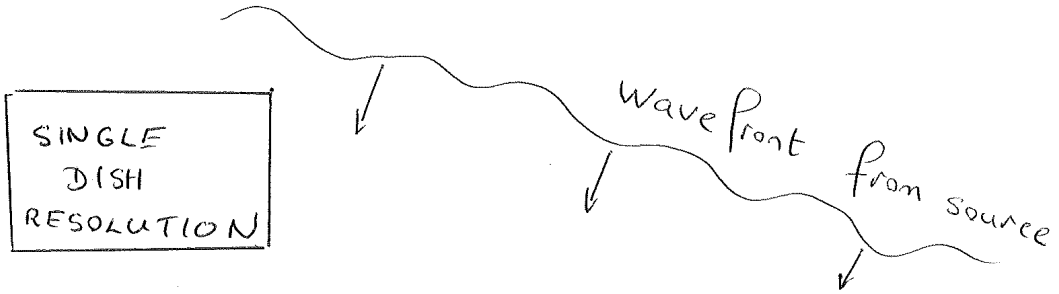

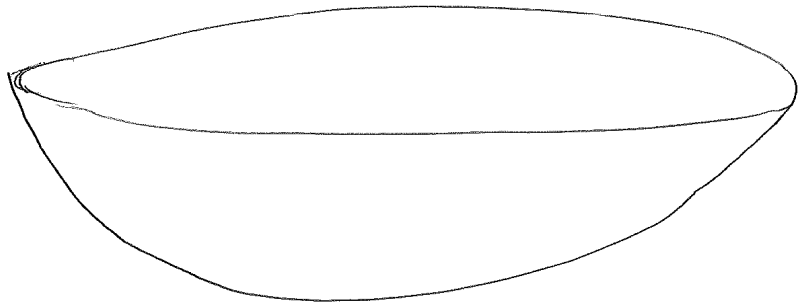

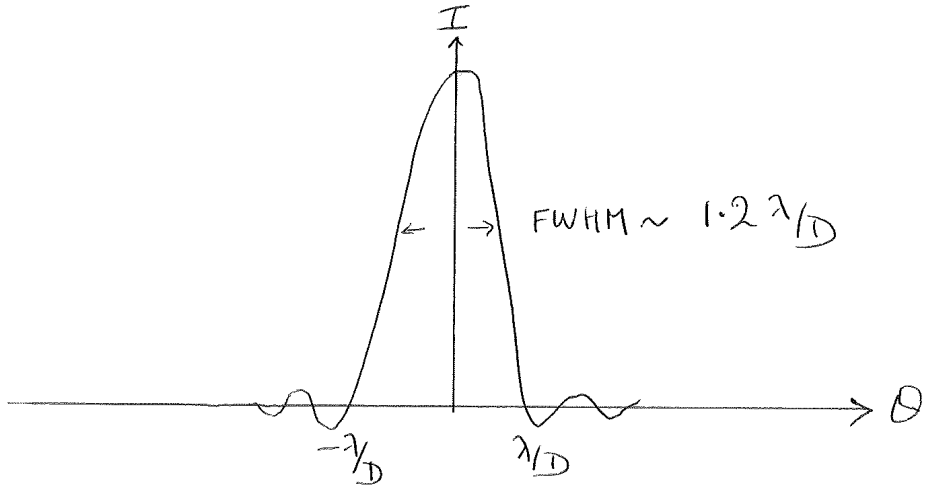

Response in sky

Resolution $\sim \lambda/D$

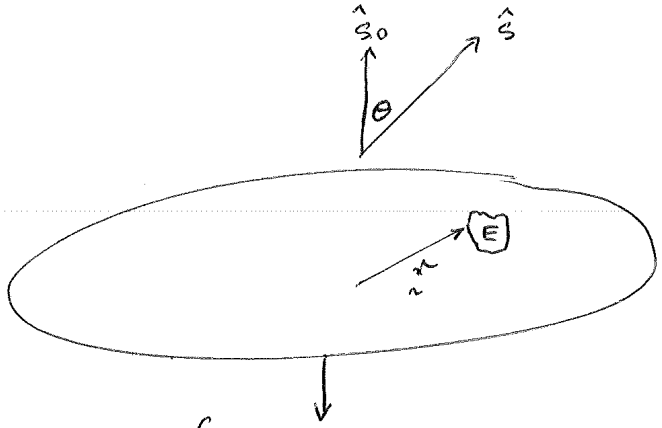

$$\text{Voltage} = \int W(r)\, E(r) \exp \frac{2\pi i}{\lambda}\, \underset{\sim}{r}\cdot\underset{\sim}{s}\; dA$$

vectors add in-phase in direction $\underset{\sim}{s}_0$

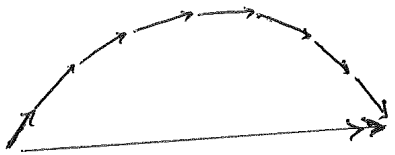

$1/2$ Power in direction $\pm \frac{1.22}{D}$

($1/\sqrt{2}$ in voltage)

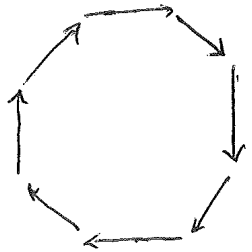

Zero Response

in direction

$\theta \sim \pm \lambda/D$

APERTURE SYNTHESIS TELESCOPES

- Build an **array** of N antennas, $(j = 1....N)$
- Measure the **average** cross correlation $< E_j E_k^* >$
  for all antenna pairs (j, k).
- Compute array response, $P(\mathbf{s})$ in direction $\mathbf{s}$

$$P(s) = \Sigma < E_j E_k^\star > \quad \exp \frac{2\pi i}{\lambda} \mathbf{b}.\mathbf{s}$$

  $\mathbf{b}$ is the vector separation of antenna pair (j, k)

  $\mathbf{s}$ is unit vector in direction of the source.

- Skeleton arrays
  T-arrays contain same relative spacings as square apertures.
- Sample different pieces of the aperture at different times.
  preserve phase across the aperture to synthesize a large telescope.

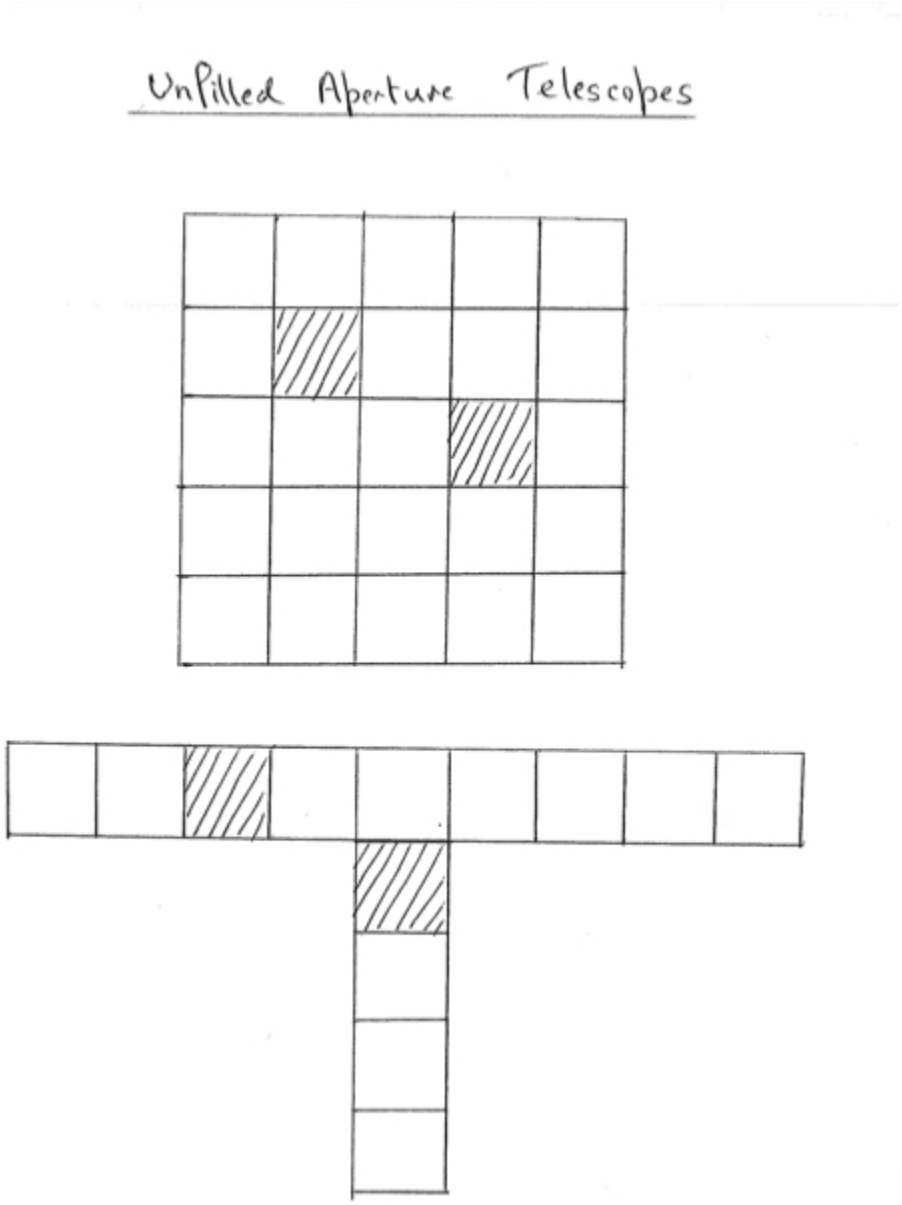

Figure 4: Aperture Synthesis: filled and unfilled apertures. The T-array contains same relative spacings as square aperture, but weighting is different.

Two element Interferometer

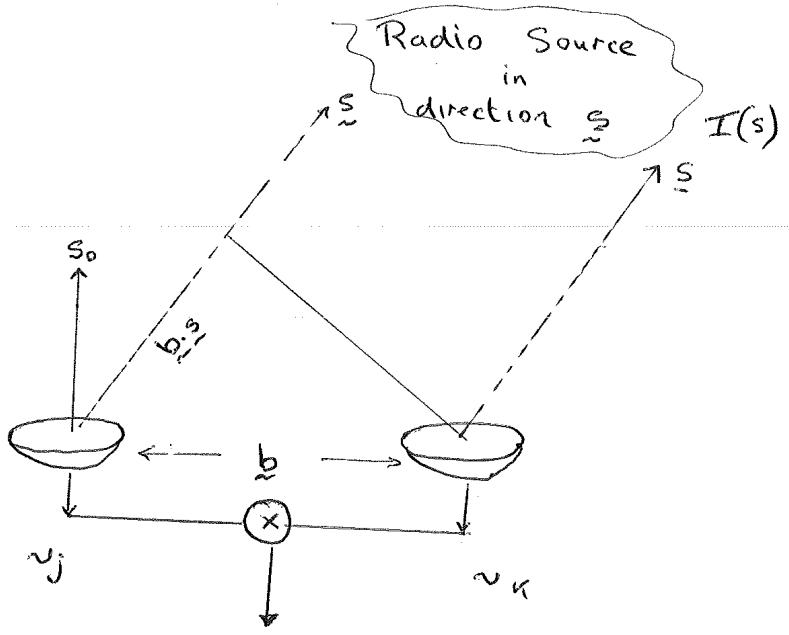

$$\text{Response} \sim v_j v_k^* \exp \frac{2\pi i}{\lambda} \underset{\sim}{b}.\underset{\sim}{s}$$

For extended radio source distribution $I(s)$

$$\text{Response} = \int_{\text{Source}} I(s) \exp \frac{2\pi i}{\lambda} \underset{\sim}{b}.\underset{\sim}{s}$$

- Response of a 2-element interferometer to point source:

$$P(s) = v_j(s)\ v_k^{\star}(s)\ \exp\frac{2\pi i}{\lambda}\mathbf{b}.\mathbf{s}$$

  $\mathbf{b}$ is the vector separation of antenna pair (j, k)

  $\mathbf{s}$ is unit vector in direction of the source.

- $\mathbf{b} = (b_N, b_E, b_Z) = (b_x, b_y, b_z) = (u, v, w)$
- $\mathbf{s} = (HA, DEC), (AZ, EL), (X, Y, Z)$
- (u,v,w) - projected antenna separation in direction $\mathbf{s}$

$$u = b_x\ sin\ h + b_y\ cos\ h$$
$$v = (-b_x\ cos\ h + b_y\ sin\ h)\ sin\ \delta + b_z\ cos\ \delta$$
$$w = (b_x\ cos\ h - b_y\ sin\ h)\ cos\ \delta + b_z\ sin\ \delta$$

Earth Rotation Aperture Synthesis

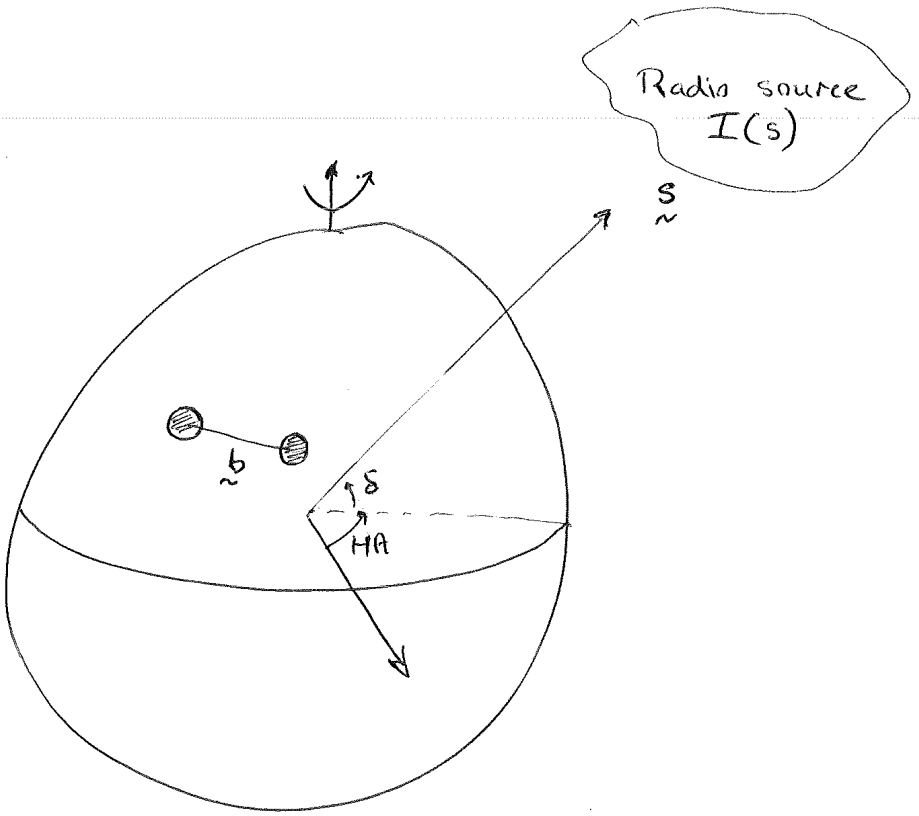

EARTH ROTATION APERTURE SYNTHESIS.

- Array of antennas track source across sky
- Measure cross correlation $< E_j E_k^* >$ for each antenna pair (j, k)
- Earth's rotation samples an ellipse in the aperture plane.

$$V(t) = \int I(s) A(s - s') \exp \frac{2\pi i}{\lambda} \mathbf{b}.\mathbf{s} \, \mathrm{ds}$$

- Antennas pointed in direction s', the pointing center.
- $A(s - s')$ is antenna area in direction s
- s_0 is phase tracking center. $\sigma = s - s_0$ is vector from s_0 to $I(s)$.

$$V(t) = \exp \frac{2\pi i}{\lambda} \mathbf{b}.\mathbf{s_0}(t) \int I(\sigma) A(s - s') \exp \frac{2\pi i}{\lambda} \mathbf{b}.\sigma \mathrm{d}\sigma$$

Instrumental terms Source structure

- If σ is small, then we write this as a 2D Fourier transform.

$$V(u,v) = \int I(x,y) A(x-x', y-y') \exp \frac{2\pi i}{\lambda}(ux+vy)\,\mathrm{d}x\mathrm{d}y$$

  $\sigma = (x, y, z)$ and $b = (u, v, w)$

- 3D transform, "w projection", or faceting is used to image large sources.
- An interferometer array is a chromatic instrument,
  - we must use a small range of λ to avoid bandwidth smearing.
  - for wideband sources, we can use multi frequency synthesis, MFS,
  - to get Fourier samples of the brightness distribution at each λ.

- We only have discrete samples of V, so we define a weighting function W, and evaluate:

$$I'(x,y) = \int W(u,v)V(u,v) \exp \frac{-2\pi i}{\lambda}(ux+vy)\,\mathrm{d}u\mathrm{d}v$$

- The weighting function W can have any value where V is sampled

  $W = 0$ where V is not sampled.

- I' is The Fourier transform of the product of V and W,

  which is the convolution of the Fourier transforms of V and W:

$$I'(x,y) = B(x,y) \star [I(x,y)A(x,y)]$$

where

$$B(x,y) = \int W(u,v) \exp \frac{-2\pi i}{\lambda}(ux+vy)\,\mathrm{d}u\mathrm{d}v$$

B is the synthesized beam - the interferometer point source response.

INTERNATIONAL ARRAY TELESCOPES: ALMA, EVLA AND LOFAR

- State of the art aperture synthesis telescopes

  at millimeter/submillimeter, centimeter and meter wavelengths:

- ALMA - Atacama Large Millimeter Array: 64 antennas.
- EVLA - Expanded VLA: 27 antennas.
- LOFAR - Low Frequency Array: with antennas at 77 stations spread over 100 km. Frequency range 30-90 and 120-250 MHz.

  Antennas at each station are combined into phased array beams to reduce the data rate to a single data stream for each station.

RADIO SOURCE STRUCTURE AND TELESCOPE DESIGN

- We need to know something about the sources of radio emission
  in order to design our telescopes and observations.
- Some of the 1st observations are usually surveys
  to determine the distribution and nature of the sources.
  Later observations study the details of sources, or classes of sources.
- Telescopes and observing techniques together
  define a matched filter to a set of possible observations
  to determine the characteristics of $I(\mathbf{s}, \nu, poln, time)$.
- Some observations are a good match to the instrument.
  Others are more difficult: "challenging", or "impossible".
  We design new instruments to match new science goals.

MILLIMETER WAVE ASTRONOMY FROM COMETS TO COSMOLOGY

Thermal emission

- Black body - planets, asteroids, quiet sun
- Dust - grey body: dust emissivity at millimeter wavelengths
- Molecular lines: rotational-vibrational transitions
- Star formation, molecular clouds, stellar envelopes, YSO, evolved stars
- Galactic structure: CO and isotopes, CS, HCN, HCO+....
- Spiral and Dwarf galaxies: structure, gas content, rotation curves
- High redshift galaxies

Non-Thermal emission

- Relativistic electrons & magnetic fields, synchrotron radiation, inverse compton, masers, cyclo-synchrotron
- SN remnants
- Radio galaxies: nuclei, radio hot spots
- Quasars, Blazars, and Seyfert galaxies.
- Active sun: Solar flares.
- Masers: SiO, CH3OH
- Pulsars: steep spectrum, not important at millimeter wavelengths
- Comets: collisional and fluorescent excitation (Solar IR photons)
- VLBI

ALMA DESIGN REFERENCE SCIENCE PLAN

- ALMA was designed to meet certain key science goals:
- High-priority projects for 3-4 years of full operation.
  - Detect line emission from CO or CII in a normal galaxy at a redshift z=3, in less than 24 hours.
  - Image gas kinematics in protostars and protoplanetary disks in nearest molecular clouds (150 pc).
  - High dynamic range images at an angular resolution of 0.1 arcsec.
- Some observations are a good match to the telescope.
- Others may be more difficult, "challenging", or "impossible".

ALMA

- International telescope in Chile at 5km altitude.
- ALMA: 50 x 12m. antennas.
- ACA: ALMA Compact Array : 12 x 7m + 4 x12m antennas.
- Resolution (λ/D_{max}): 5 mas - 3 arcsec.
- Primary beam (λ/D_{ant}): 9 - 56 arcsec.
- Largest scale (λ/D_{min}): 6 - 37 arcsec.
- Receiver bands: 3(84-116), 6(211-275), 7(275-373), 9(602-720) GHz.
- Future bands: 4(125-169), 5(163-211), 8(385-500), 10($\sim$ 920) GHz.
- 8 GHz bandwidth. Dual Polarization all bands.

Figure 7: ALMA array of 16 antennas.

CARMA

- University Research Observatory.
- Combined OVRO, BIMA, and SZA arrays on high site.
- 6 x 10.4m + 9 x 6.1m + 8 x 3.5m antennas.
- 23-antenna array at 2.2 km altitude in Inyo mountains CA.
- Resolution (λ/D_{max}): 120 mas - 30 arcmin.
- Primary beam (λ/D_{ant}): 25 arcsec - 1 degree.
- Largest scale (λ/D_{min}): 25 arcsec - 1 degree.
- High spatial dynamic range: 3.5m to 2km.
- Receiver bands: 26-36, 80-115, and 215-270 GHz.
- 8 GHz bandwidth. Dual Polarization in λ 1.3 mm band

Figure 8: The CARMA 23-element interferometer at Cedar Flat.

Owens Valley Array

BIMA Array

Moving 6m Telescopes from Hat Creek

Antennas arrive at CARMA site

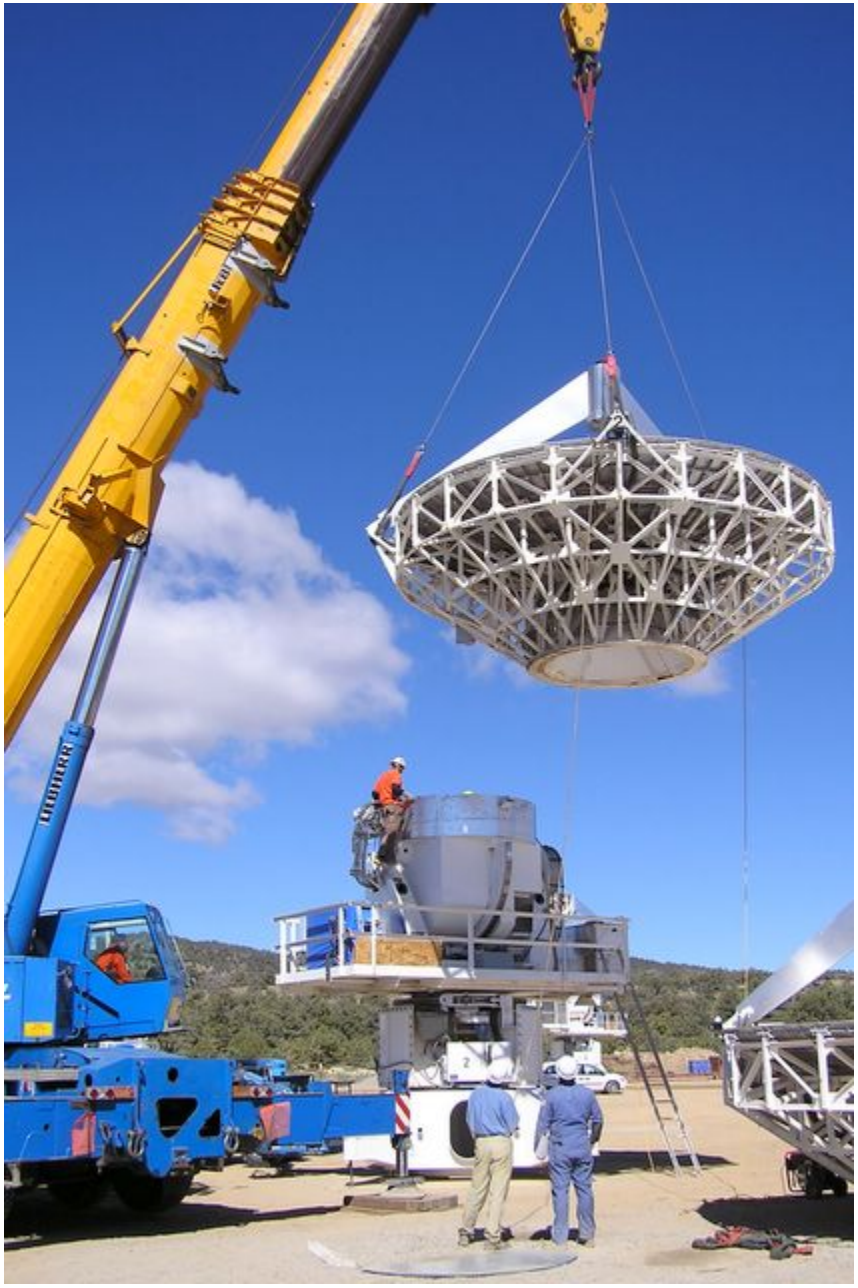

Figure 13: Re-building 6m antennas at CARMA

Moving 10m Telescopes from Owens Valley

Figure 15: Moving 10m antennas thro the narrows to CARMA

Figure 16: Re-building 10m antennas at CARMA

ANTENNA CONFIGURATIONS

- Antennas are moved to provide different resolutions.
- Large sources need compact arrays with short spacings.
- High resolution needs extended arrays with large spacings.
- Spatial Dynamic Range – range of angular scales mapped.
  $\sim \lambda/D_{min} - \lambda/D_{max}$
- Structure $> \lambda/D_{min}$ or $< \lambda/D_{max}$ is not mapped.
- CARMA has antenna spacings $\sim$ 3.5m to 2 km.
- ALMA has antenna spacings $\sim$ 15m to 15 km.
- ACA - ALMA compact array has spacings $\sim$ 8m to 80m.

Figure 17: E-configuration

IMAGE FIDELITY

- Image fidelity improves as the uv sampling density is increased.
- Short spacings sample large scale structure.
- Large spacings sample small scale structure.

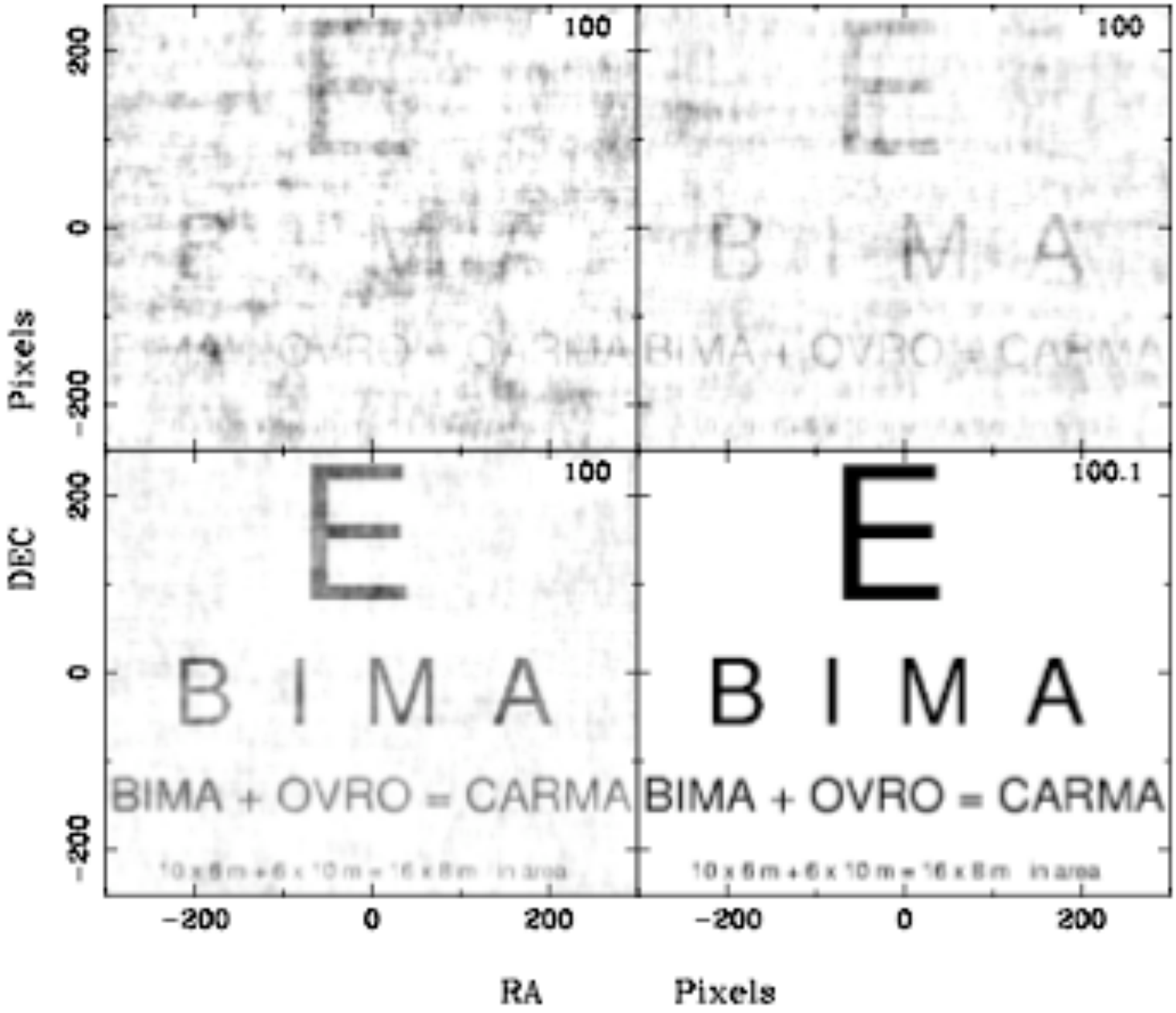

Fig. 5. Effect of uv sampling on image fidelity with 5000 (top left), 10^4 (top right), 10^5 (bottom left) and 10^6 (bottom right) uv points

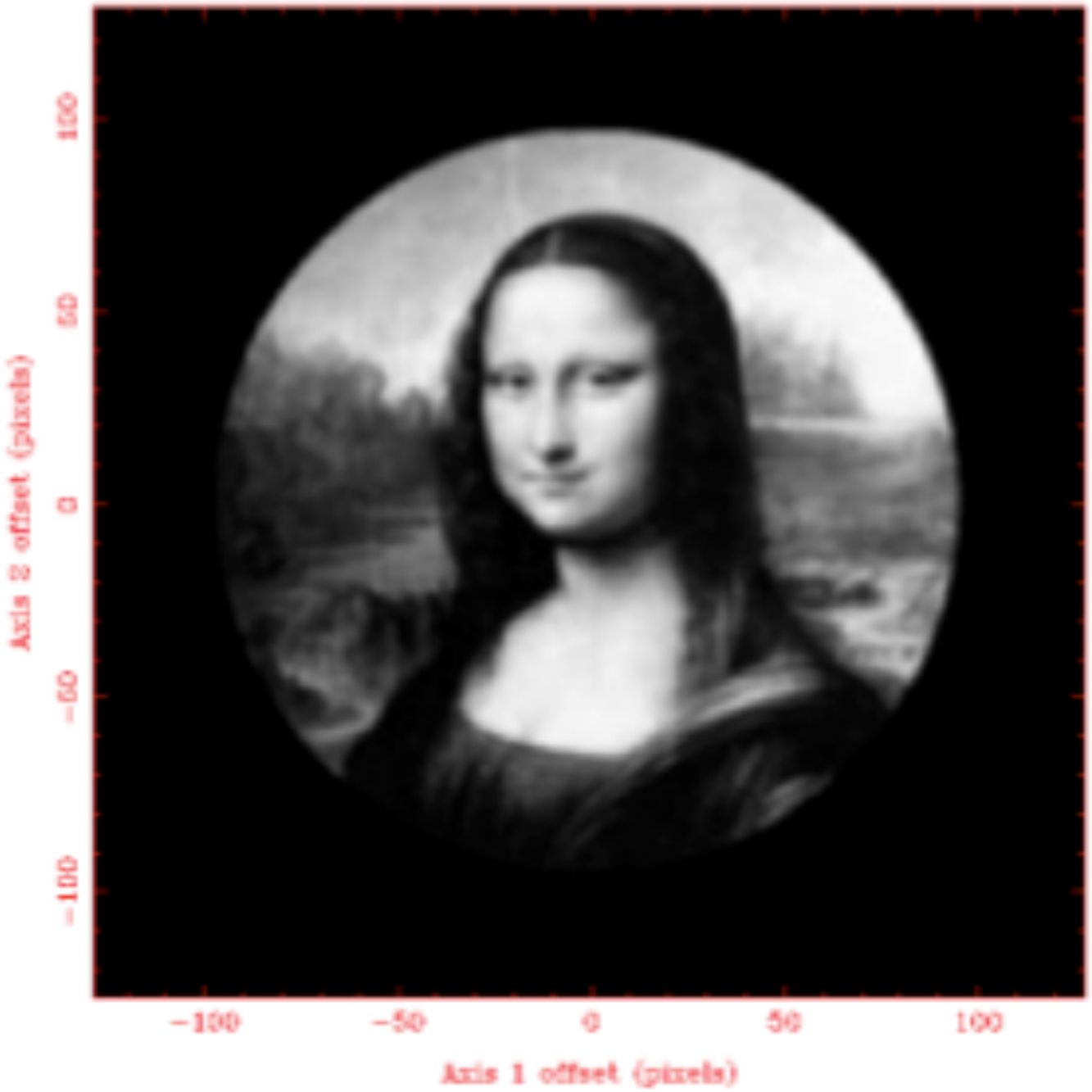

Figure 19: MonaLisa

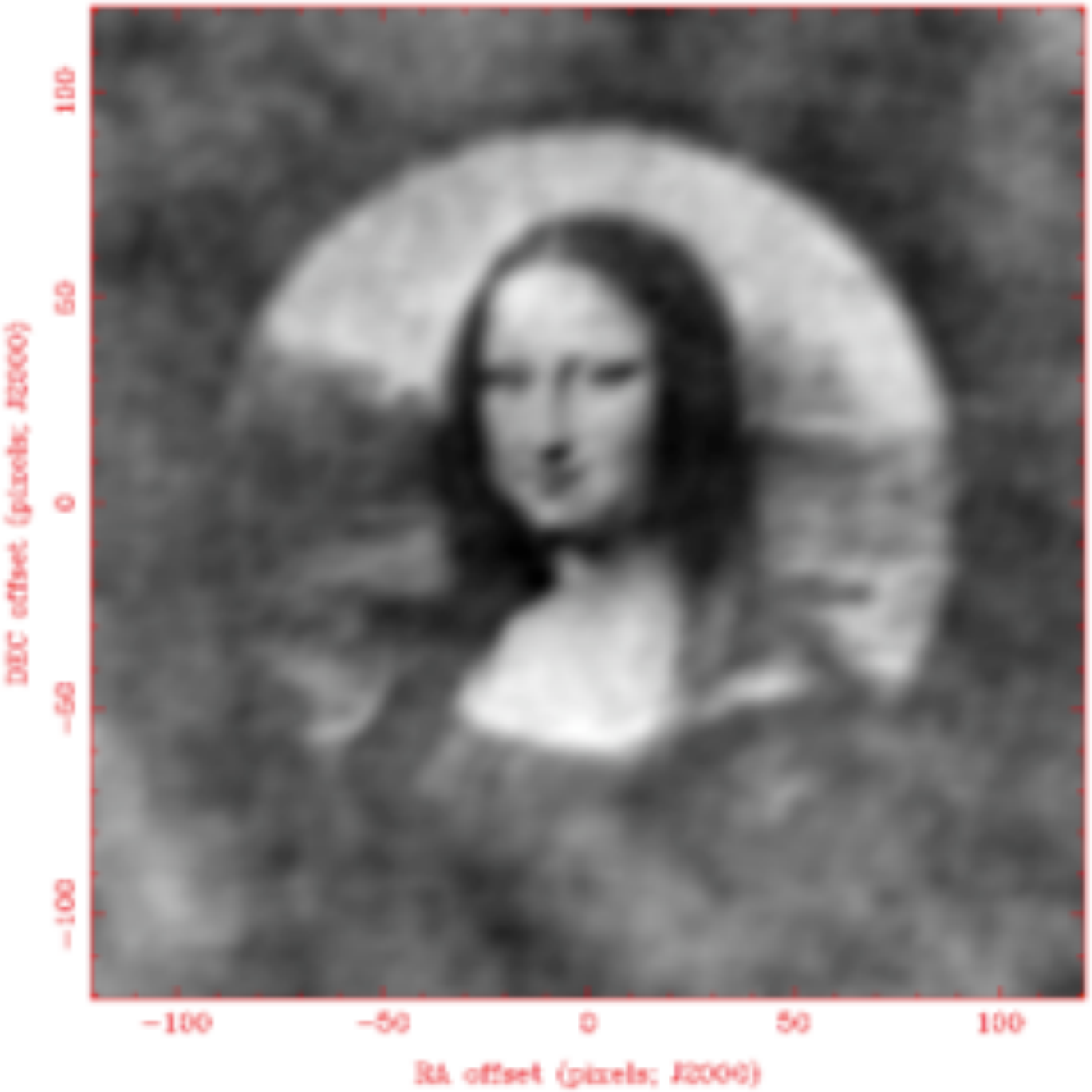

Figure 3: Image obtained with ATA-32 sampled at 1 hour intervals.

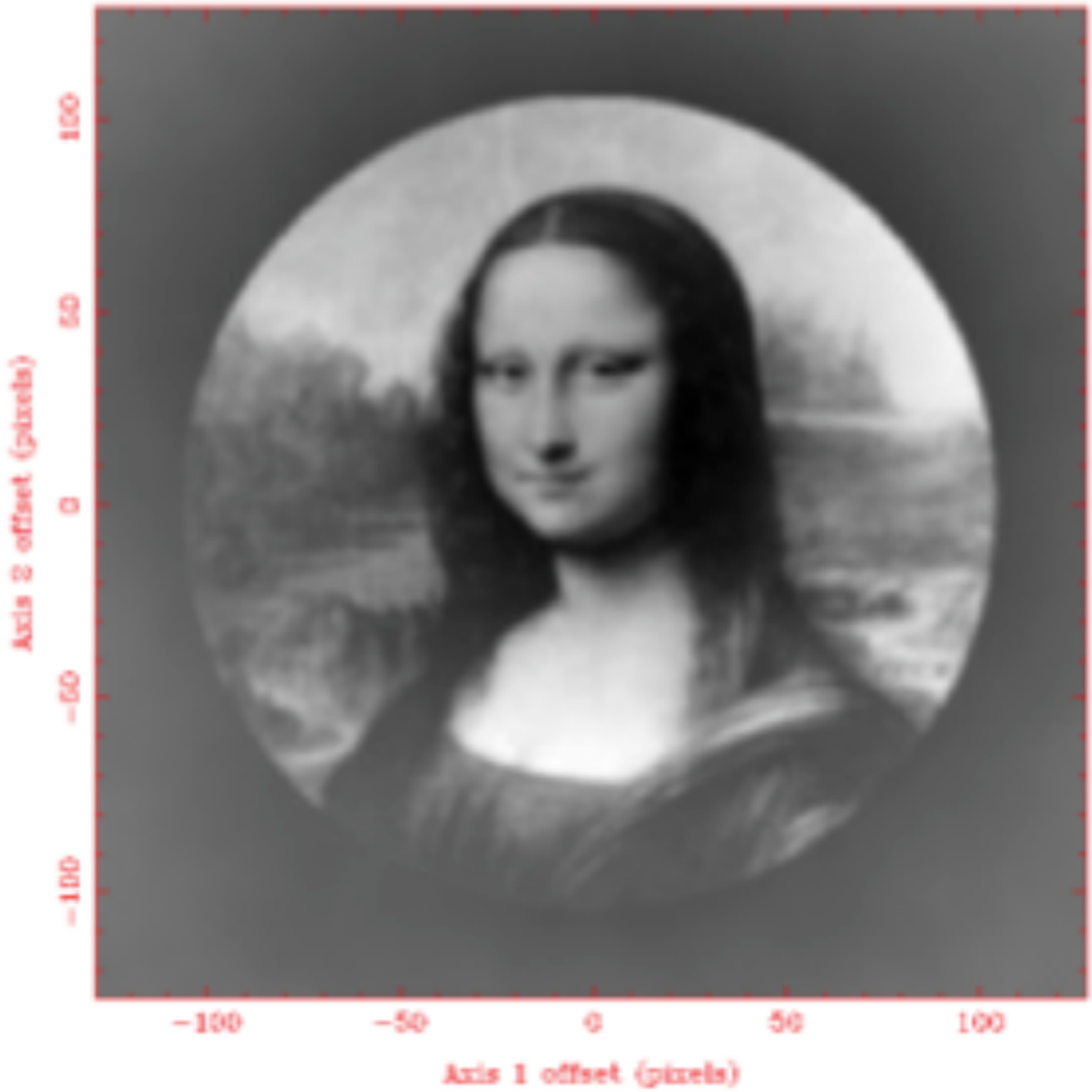

Figure 2: Image obtained with ATA-350 sampled at 1 hour intervals.

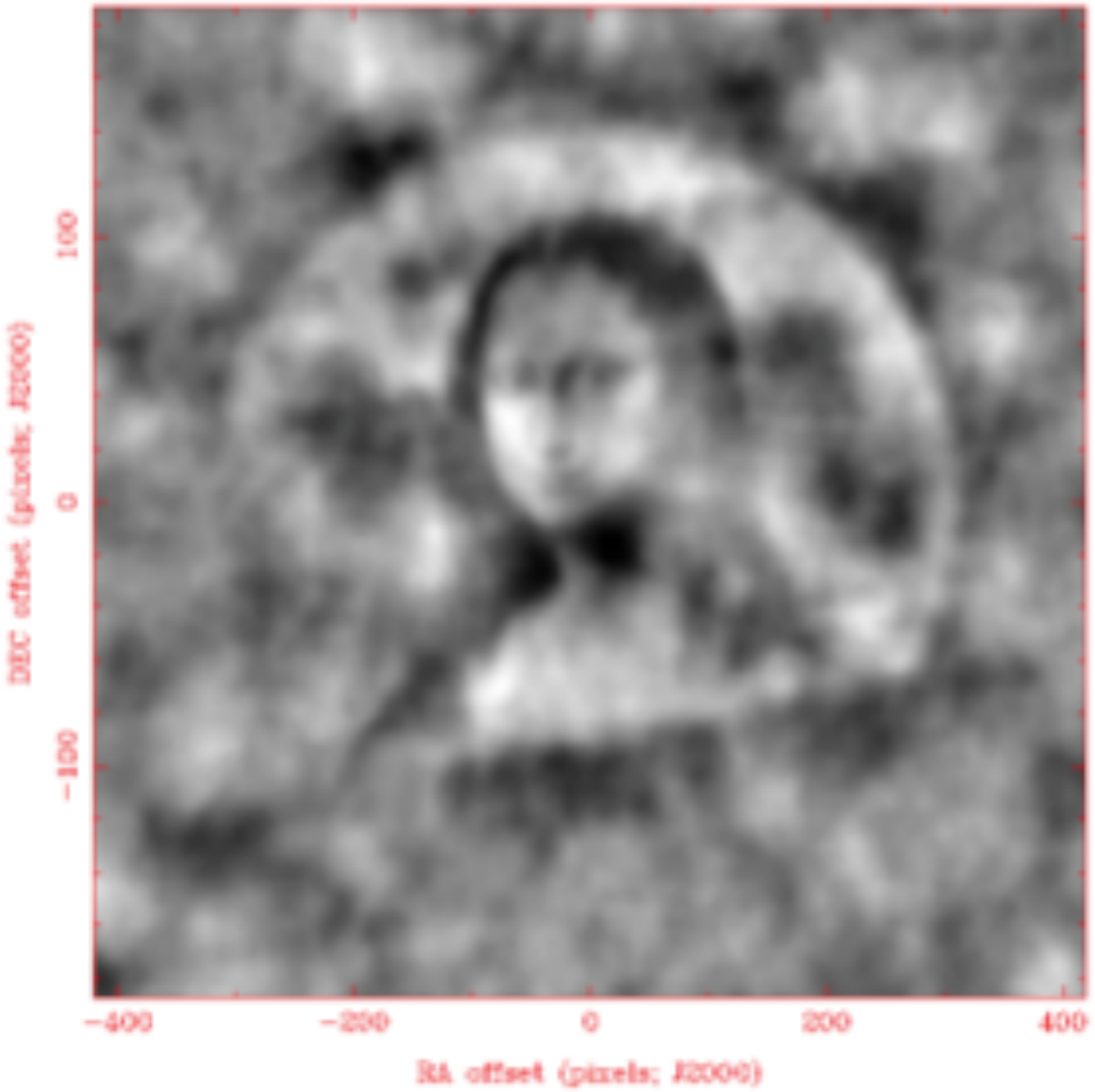

Figure 4: Image obtained with VLA-D sampled at 1 hour intervals.

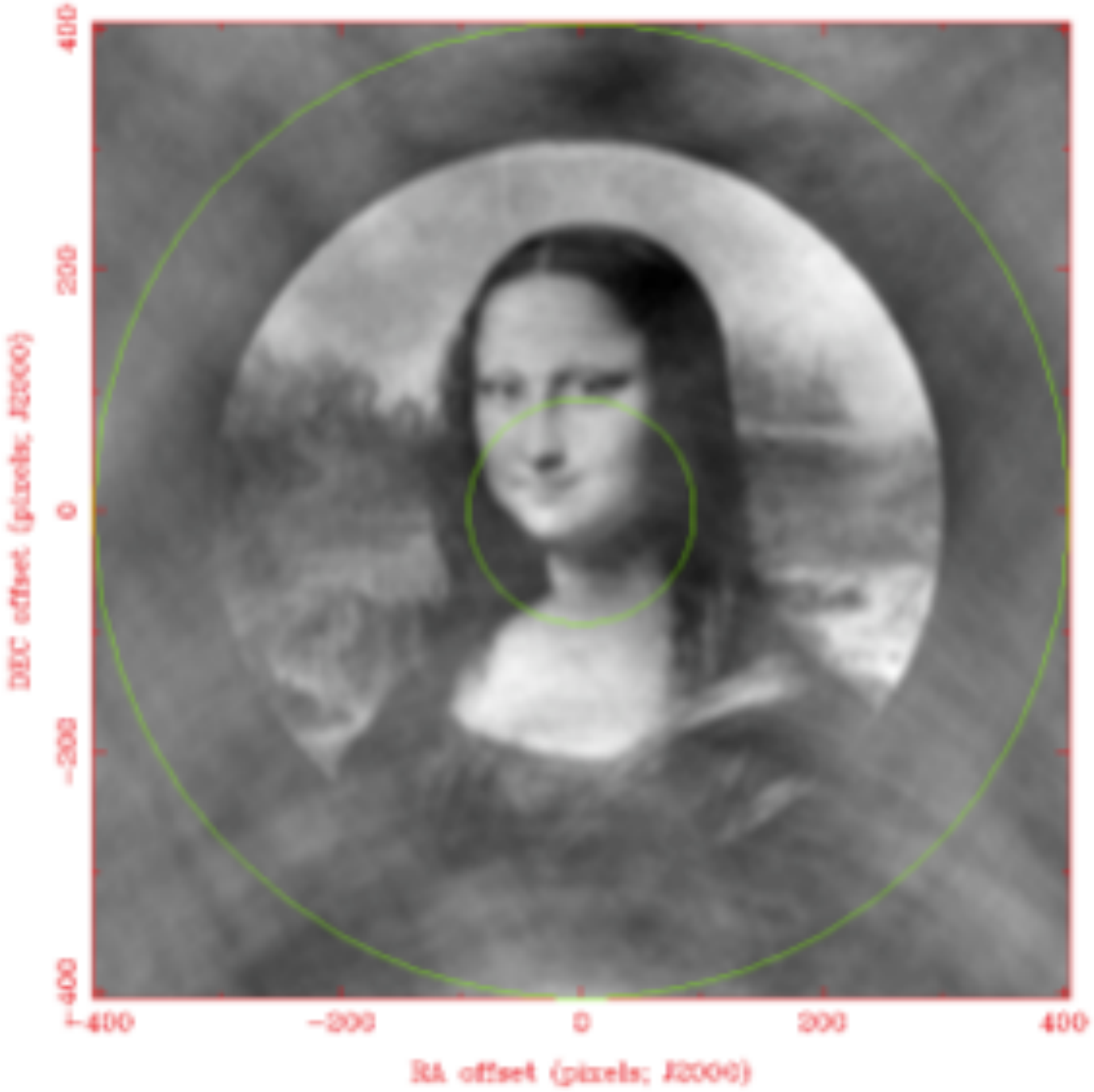

Figure 6: Image obtained with VLA-D sampled at 2 minute intervals.

IMAGE DECONVOLUTION

- Images deconvolved to remove response of the synthesized beam, B.
- Two different deconvolution algorithms are commonly used:

  CLEAN - an iterative point source subtraction algorithm, which is well matched for deconvolving compact source structures.

  MAXIMUM ENTROPY - a gradient search algorithm, to optimize the fit to an a-priori image, with a least squares fit to uv data.

HETEROGENEOUS ARRAYS

- Heterogeneous array produces better image fidelity than homogeneous array with the same number of antennas.
- Cross correlation of 3.5, 6.1 and 10.4 m antennas sample a large range of angular scales.
- CARMA large range of spacings makes high fidelity images.
- 3.5 m antennas image large scale structures, and double the density of uv samples which improves the image fidelity.
- ALMA has 12m and 7m antennas, but no 7m x 12m correlations.

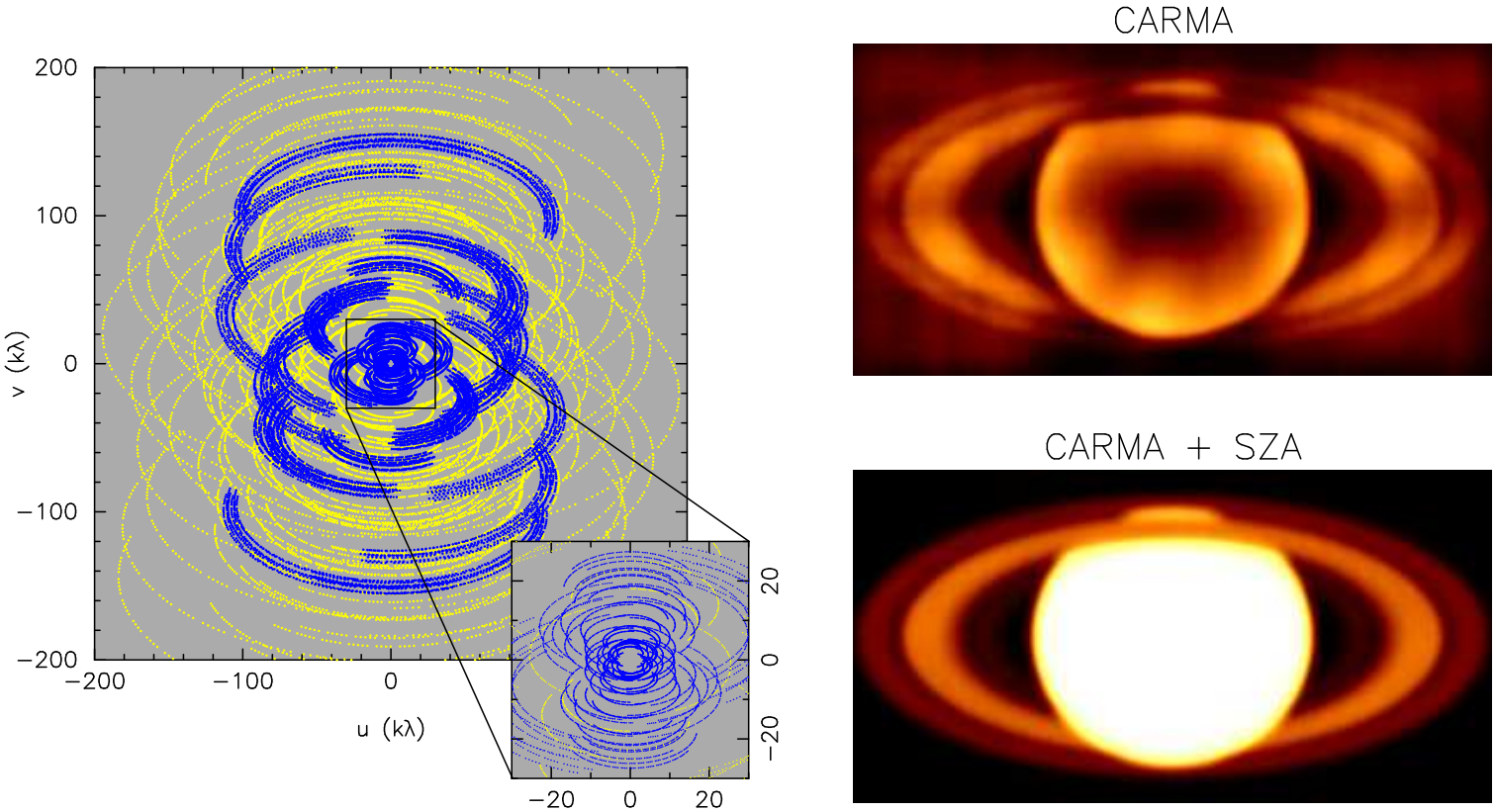

Figure 24: CARMA 23-element heterogeneous array. Left: uv data sampling at 100 GHz , DEC=30 . Yellow points: uv coverage for the CARMA 15-element array; blue points show the additional uv coverage when the 3.5-m antennas are used in the 23-element array. The dense uv sampling at short spacings shown in the inset, gives sensitivity to larger scale structure. Right: Simulated CARMA observations of Saturn show the increase in image fidelity for extended sources provided by the 3.5 m antennas.

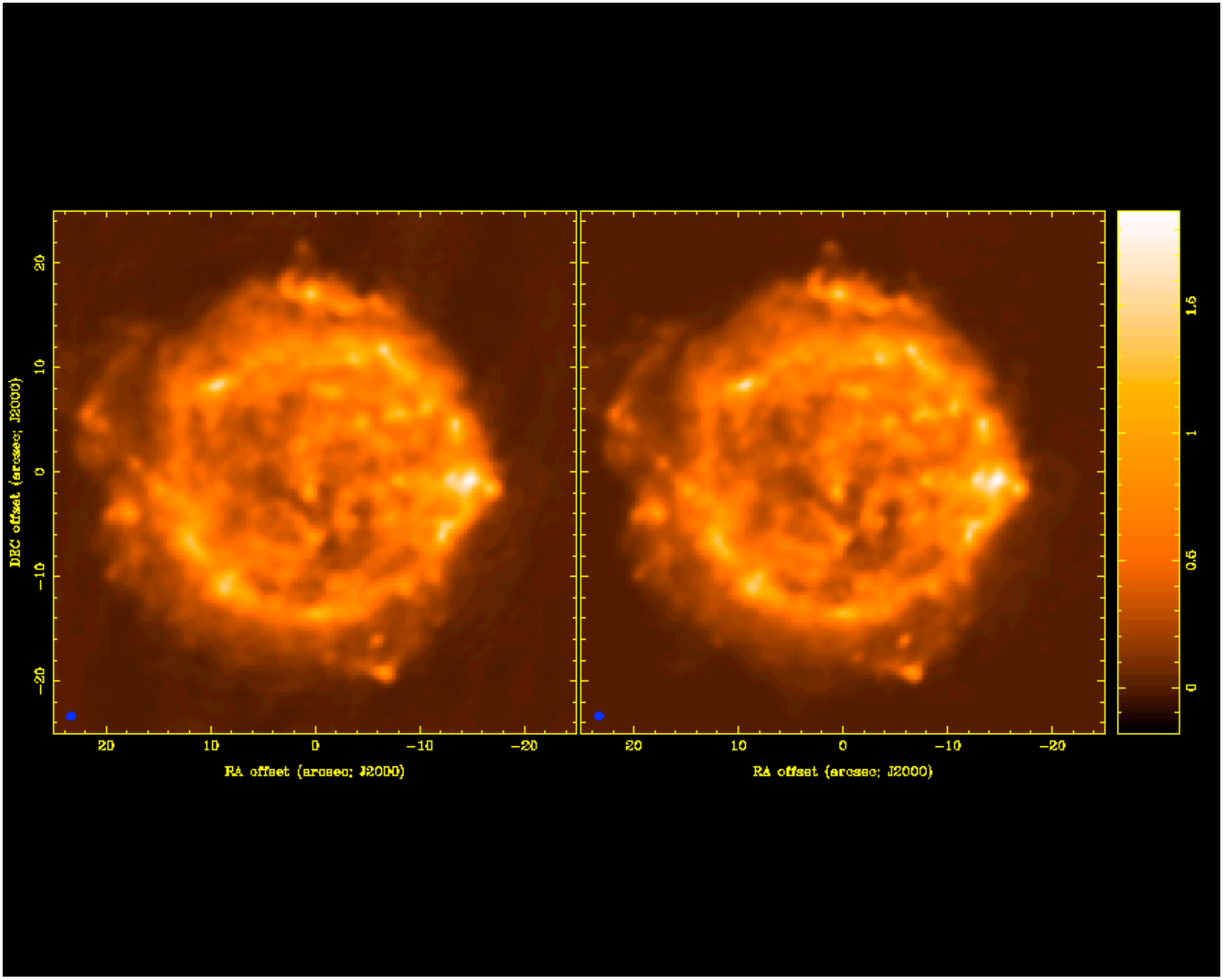
DEC offset (arcsec; J2000)
20
10
0
−10
−20
RA offset (arcsec; J2000)
20
10
0
−10
−20
RA offset (arcsec; J2000)
20
10
0
−10
−20
1.5
1
0.5
0

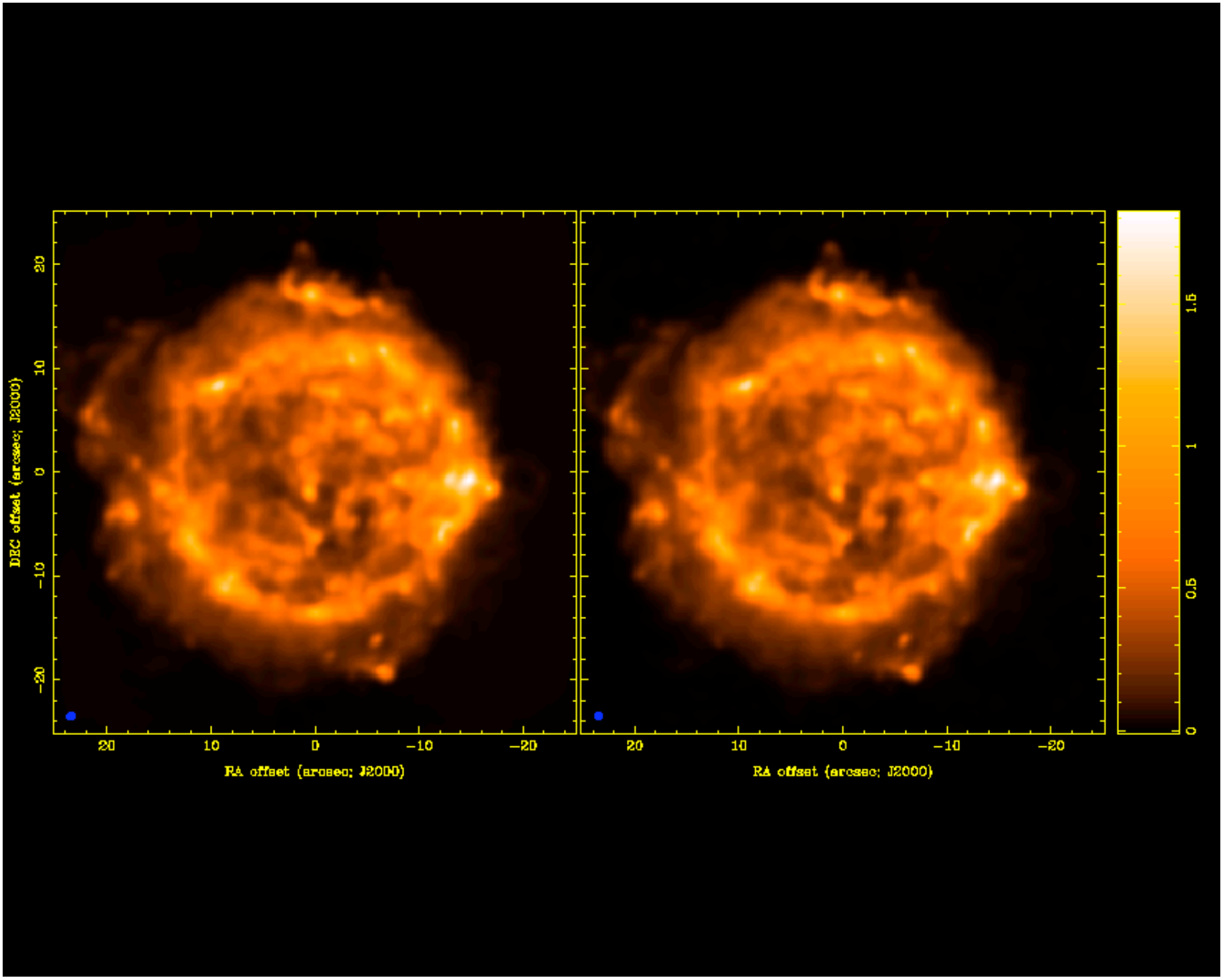
DEC offset (arcsec; J2000)
20
10
0
−10
−20
RA offset (arcsec; J2000)
20
10
0
−10
−20
RA offset (arcsec; J2000)
20
10
0
−10
−20
1.5
1
0.5
0

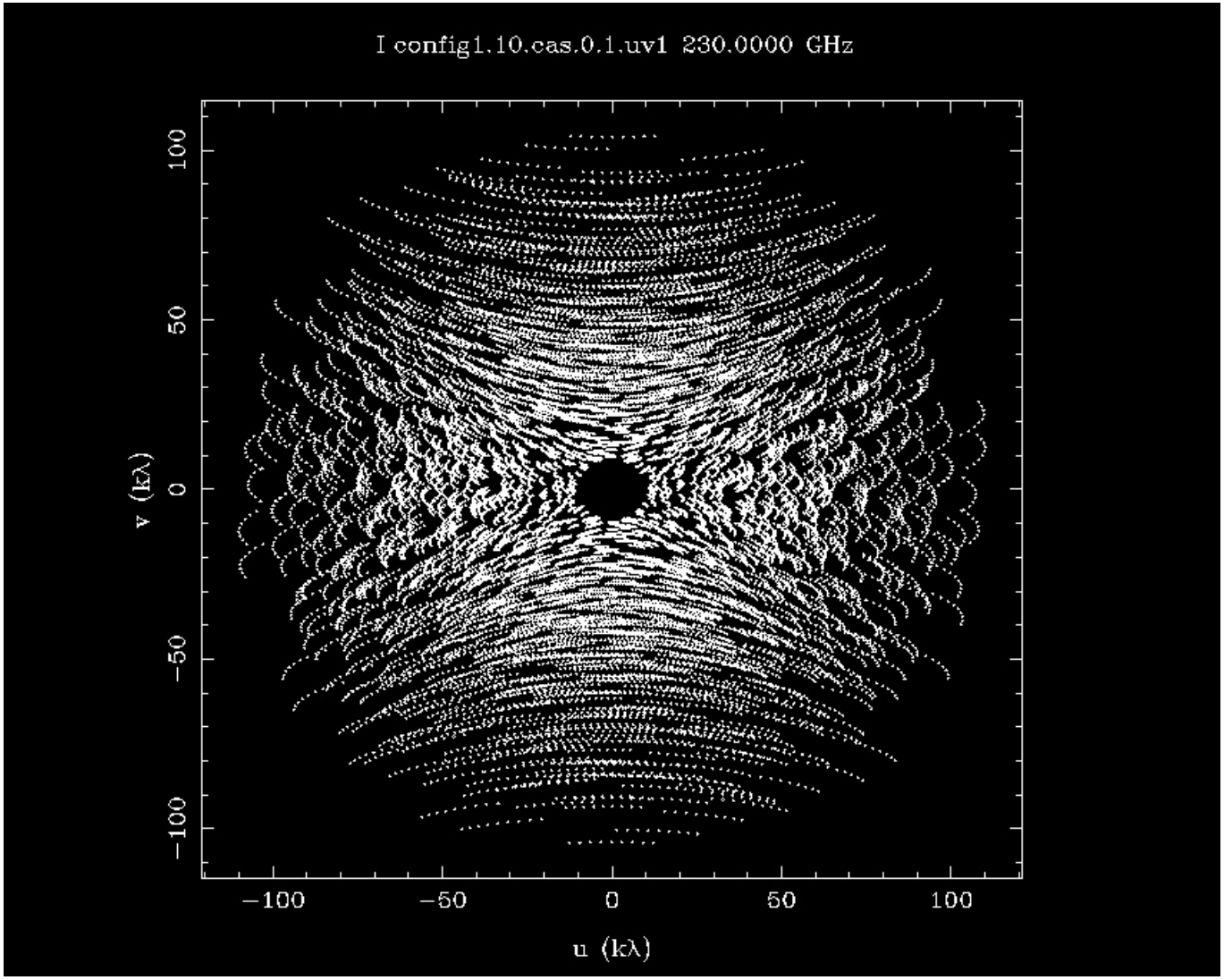

Figure 27: ALMA config1 at 10 degrees with 64-antenna configuration

ATMOSPHERIC PHASE FLUCTUATIONS

- Water vapor causes path length variations across telescope array.
- ALMA uses **rapid switching** between target and calibrator, and **water vapor radiometers** to calibrate long baselines.
- CARMA uses **Paired Antennas** observing target and calibrator.
- 3.5m antennas simultaneously observe calibrators at λ 1cm.
- Calibration sources within 1-3 degrees of target source, and antenna pairs within $\sim$ 20m so atmospheric phase fluctuations are correlated.
- Phase at λ 1cm measured by 3.5m antennas, scaled by frequency, corrects atmospheric phase on target source.
- PACS allows imaging at 0.1 arcec resolution.

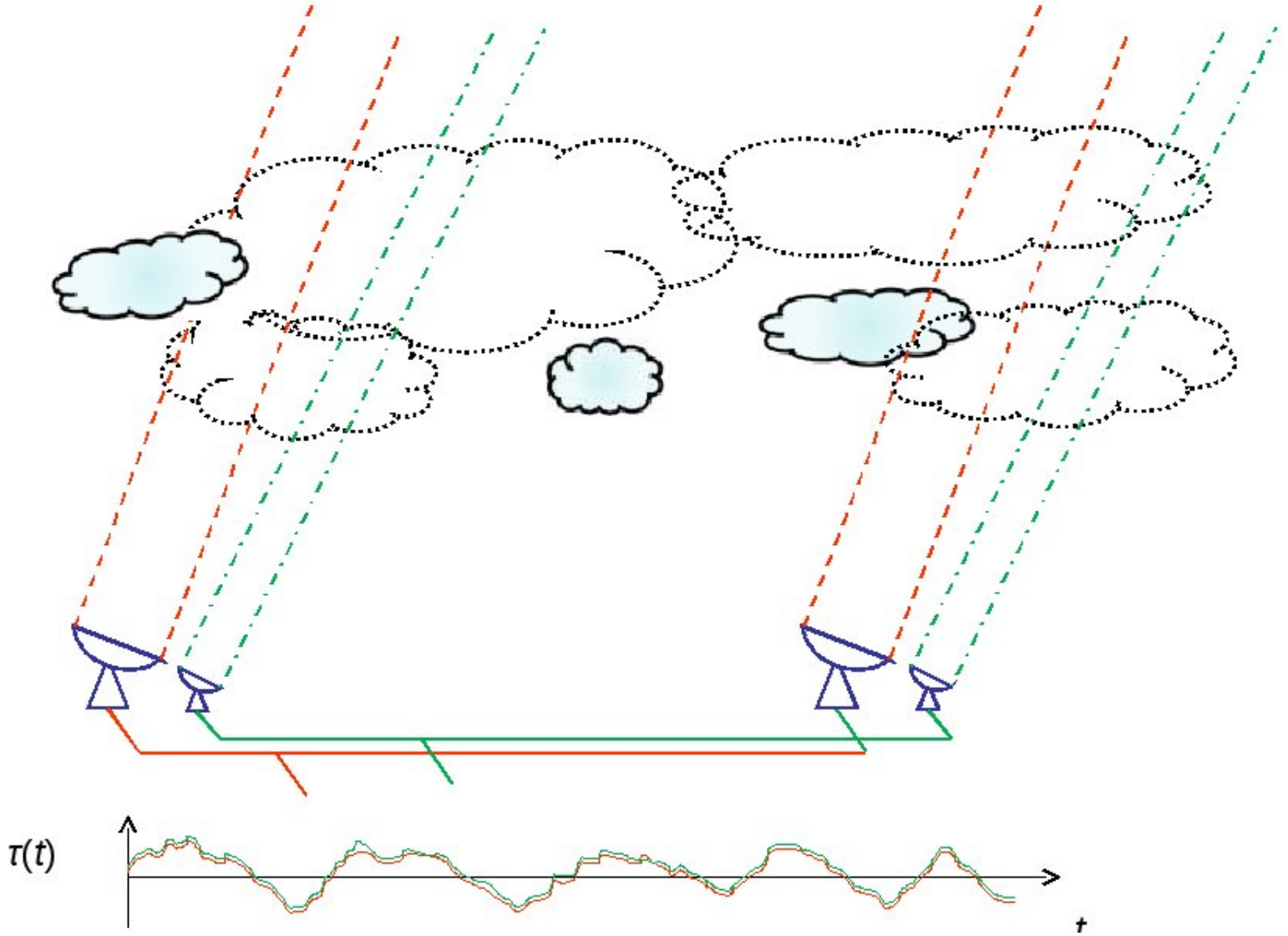

Figure 28: Paired Antenna Calibration System using 3.5 m antennas at 30 GHz. The 3.5 m antennas are paired with 6.1 and 10.4m antennas making science observations at millimeter wavelengths. The 3.5 m antennas simultaneously observe calibration sources in the 1 cm band. For calibration sources within a few degrees, the millimeter wavelength observations of the science target source, and the observations of the calibrator at 1cm, sample similar atmospheric phase fluctuations, allowing us to correct for the atmospheric phase fluctuations on long baselines at millimeter wavelengths.

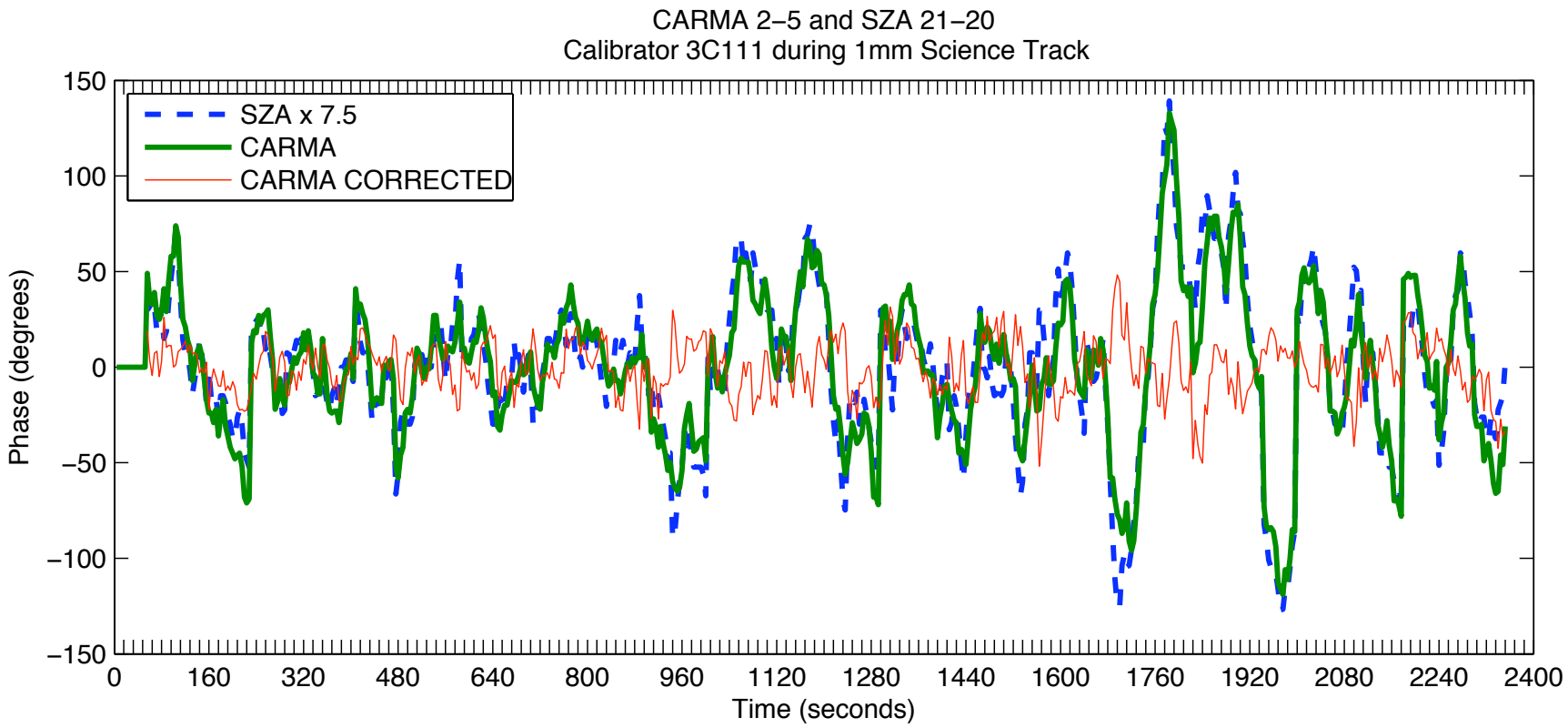

Figure 29: Phase correction using Paired Antenna Calibration System. The thick (green) line plots the phase versus time measured between CARMA antennas 2 and 5 while observing the radio source 3C111 at 225 GHz. The large phase fluctuations are caused by atmospheric turbulence on the long baseline between antennas 2 and 5. The dashed (blue) line plots the phase between two 3.5 m antennas which are close to CARMA antennas 2 and 5, but observing at 30 GHz. The 30 GHz phase multiplied by 7.5 (225/30), closely follows the 225 GHz phase allowing us to correct the 225 GHz phase. The thin (red) line shows the 225 GHz phase, corrected for atmospheric phase fluctuations.

Paired Antennas 6m + 3.5m

Paired Antennas 10m + 3.5m

CARMA map
1mm
0.3" resolution

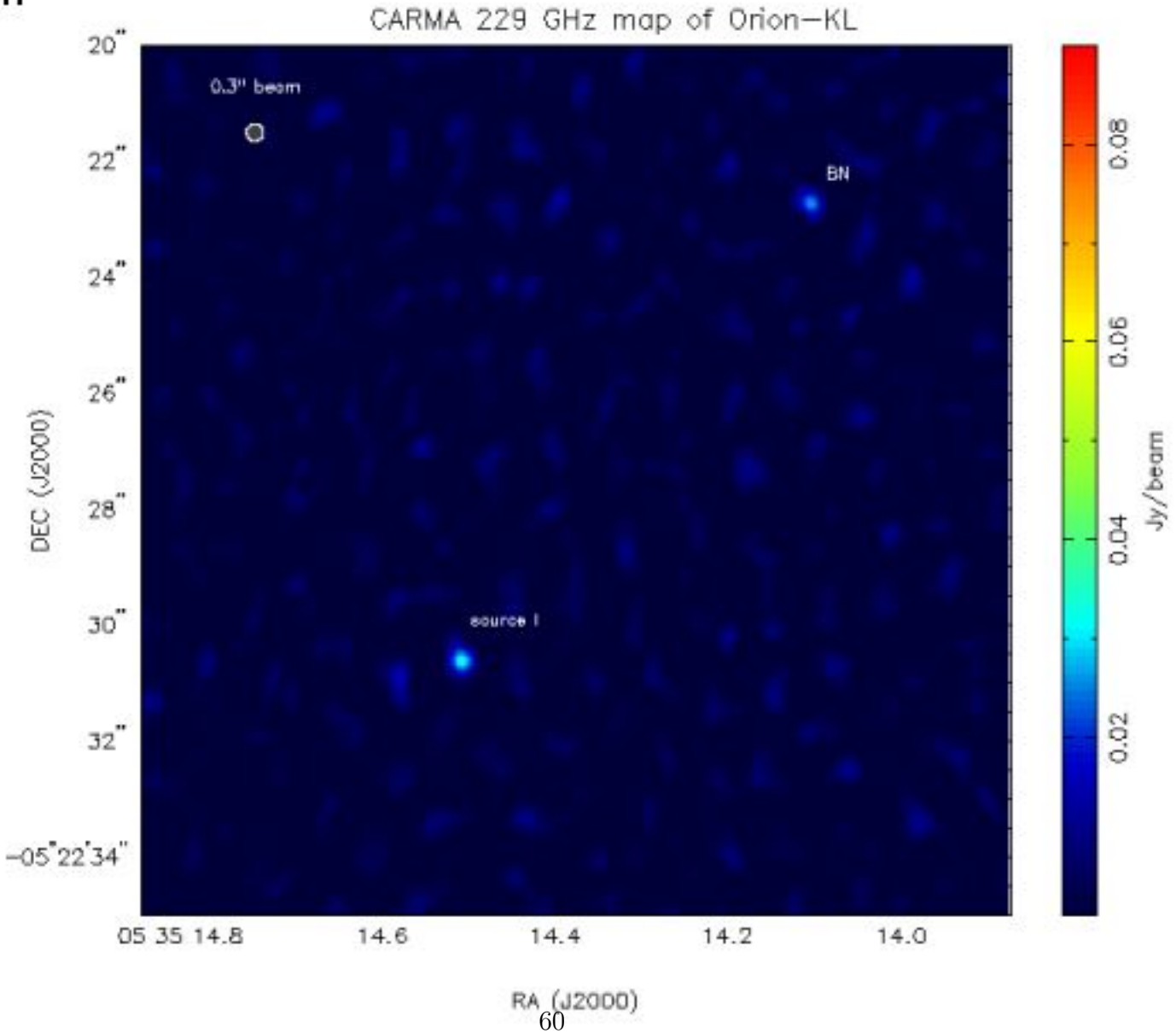

CARMA map
1mm
0.3" resolution

Ori KL source I and BN after

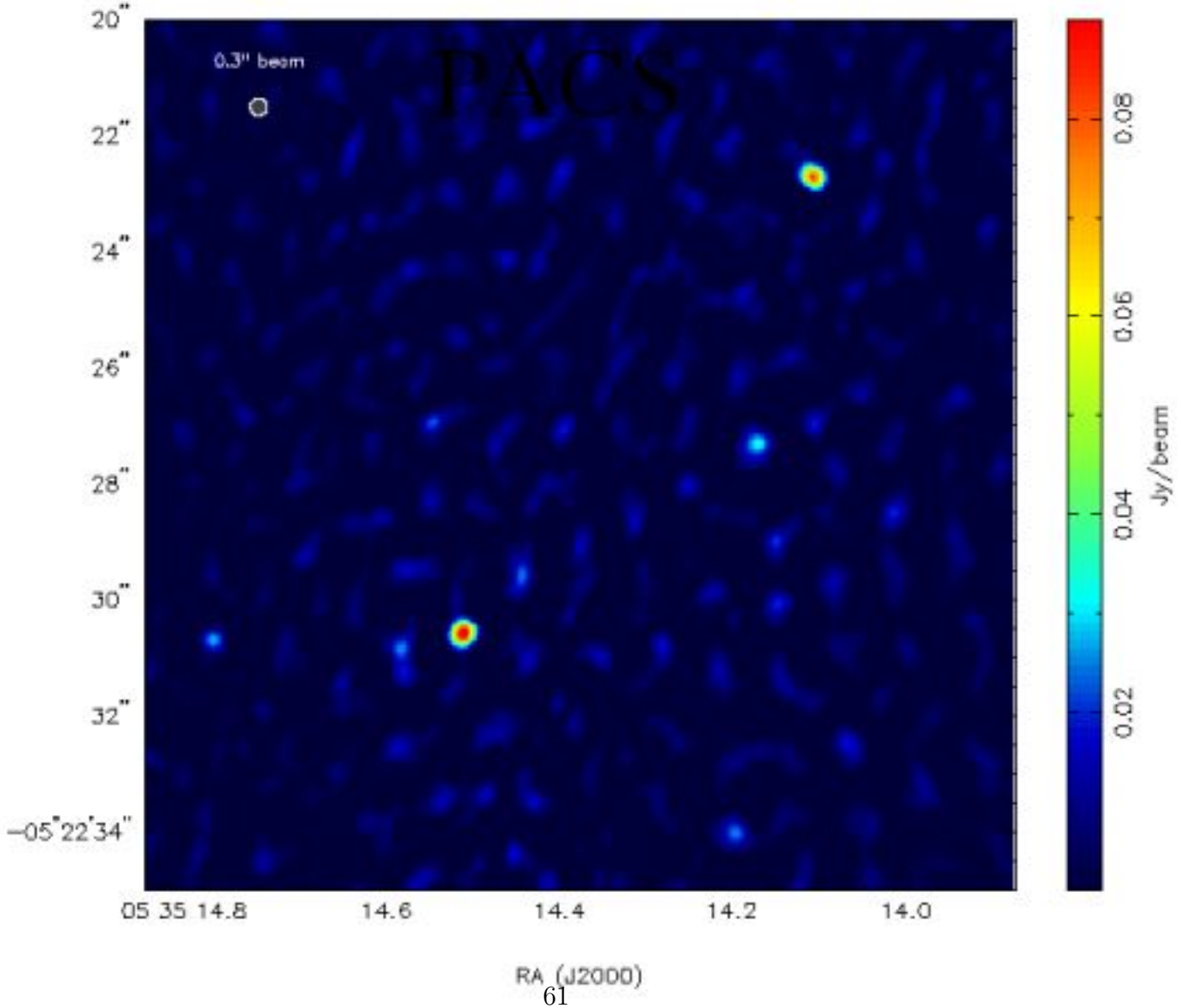

SUMMARY

- Images of the radio intensity

$$I(\mathbf{s}, \nu, polarization, time)$$

- Synthesized Image, I'

$$I' = (I \times PrimaryBeam) * SynthesizedBeam + Noise$$

- Primary Beam tracks the Sky Brightness Distribution, I
- Synthesized Beam – point spread function for aperture synthesis
- Noise from receivers, telescope, spillover and atmosphere.

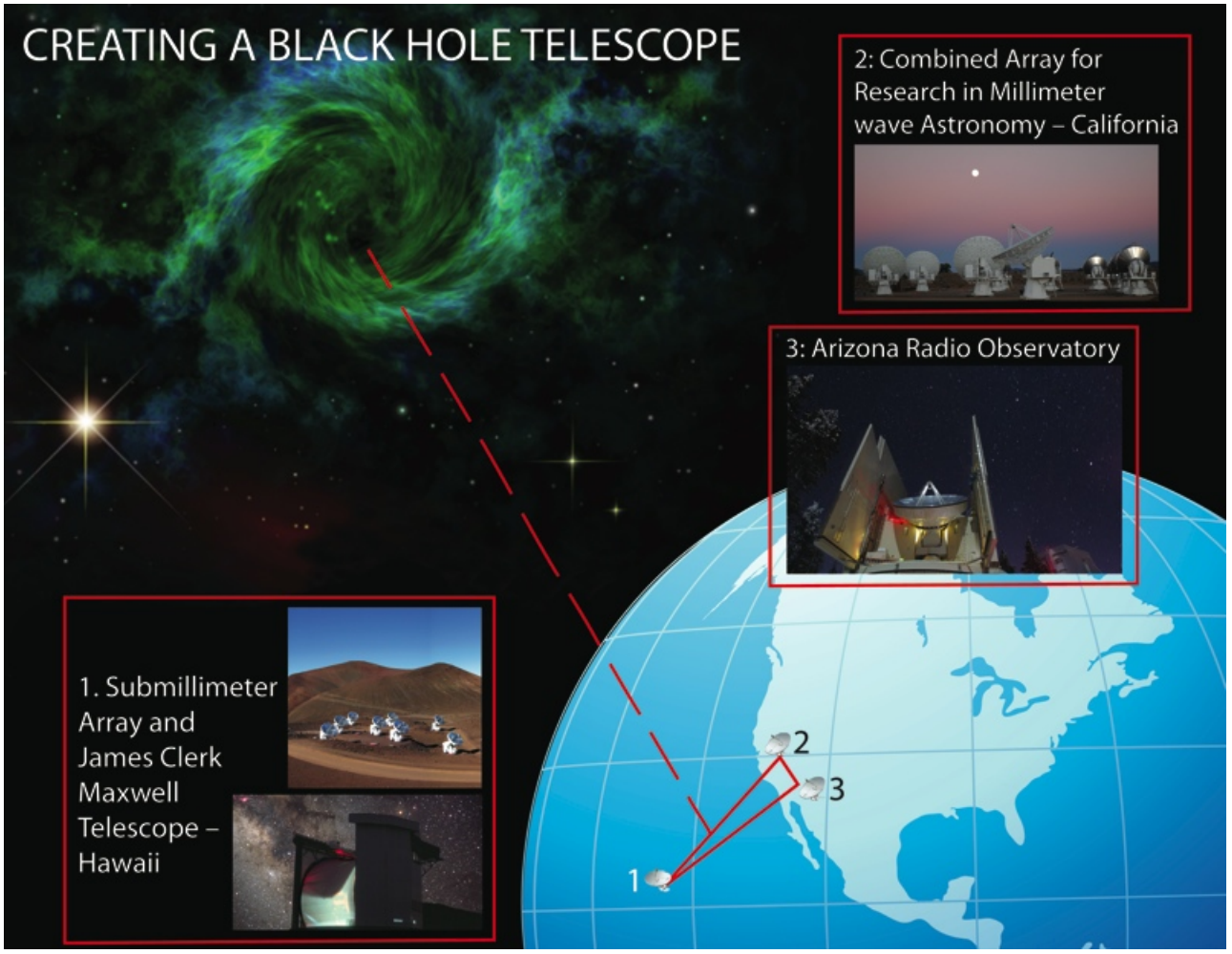

Figure 34: VLBI overview

Resolving Rsch-scale structures

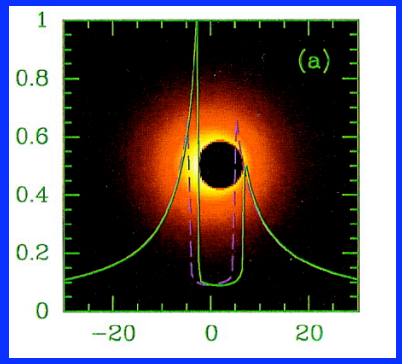

Spinning (a=1)

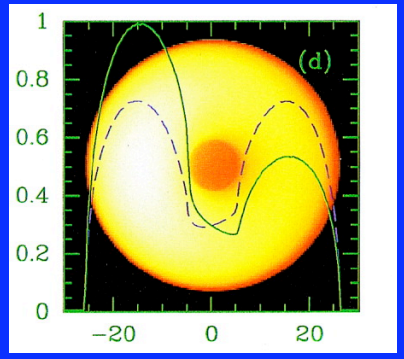

Non-spinning (a=0)

Falcke
Melia
Agol

- SgrA* has the largest apparent Schwarzschild radius of any BH candidate.
- Rsch = 10μas
- Shadow = 5.2 Rsch (non-spinning)
  = 4.5 Rsch (maximally spinning)

Figure 35: SgrA Black Hole

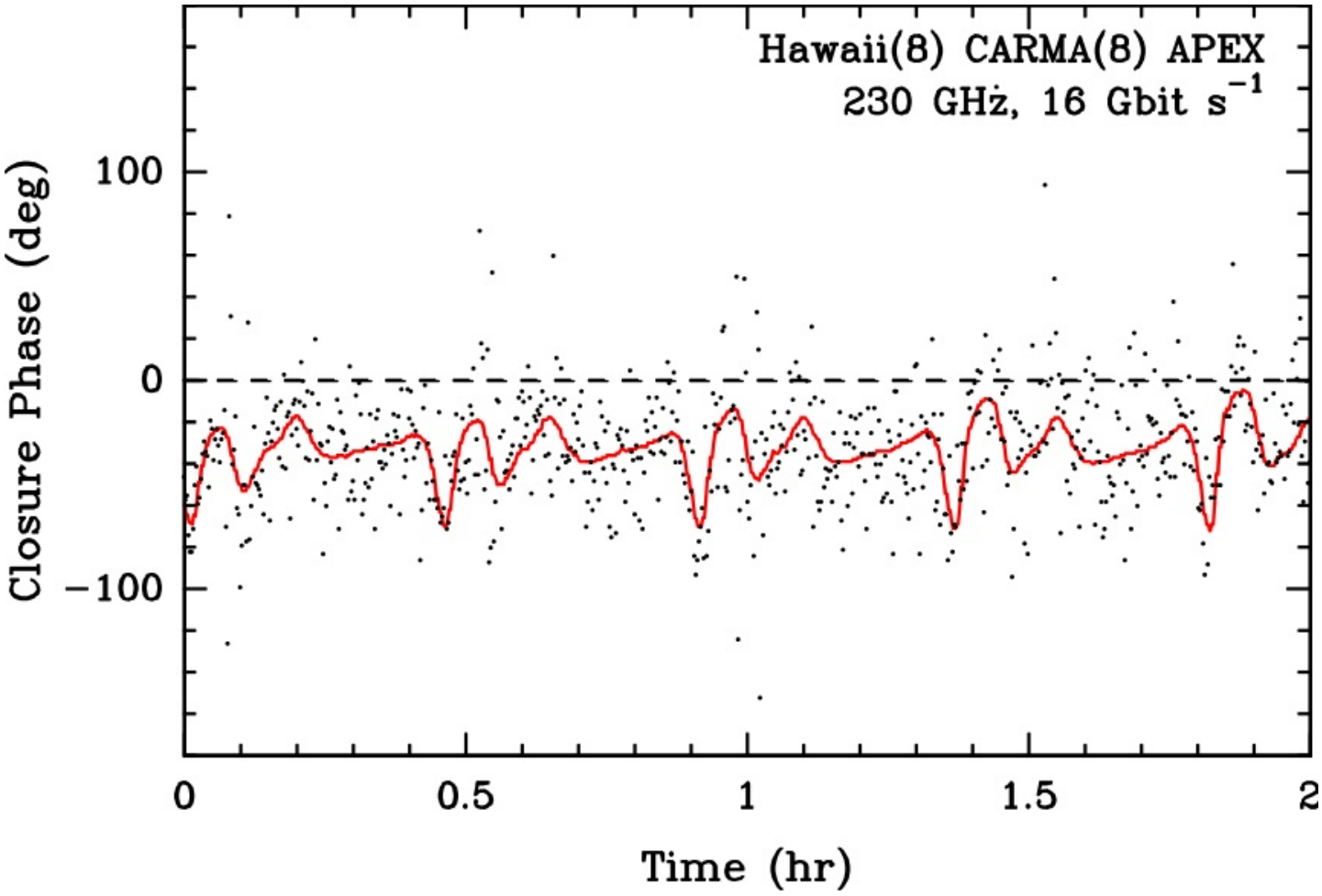

Figure 36: Closure Phase with APEX

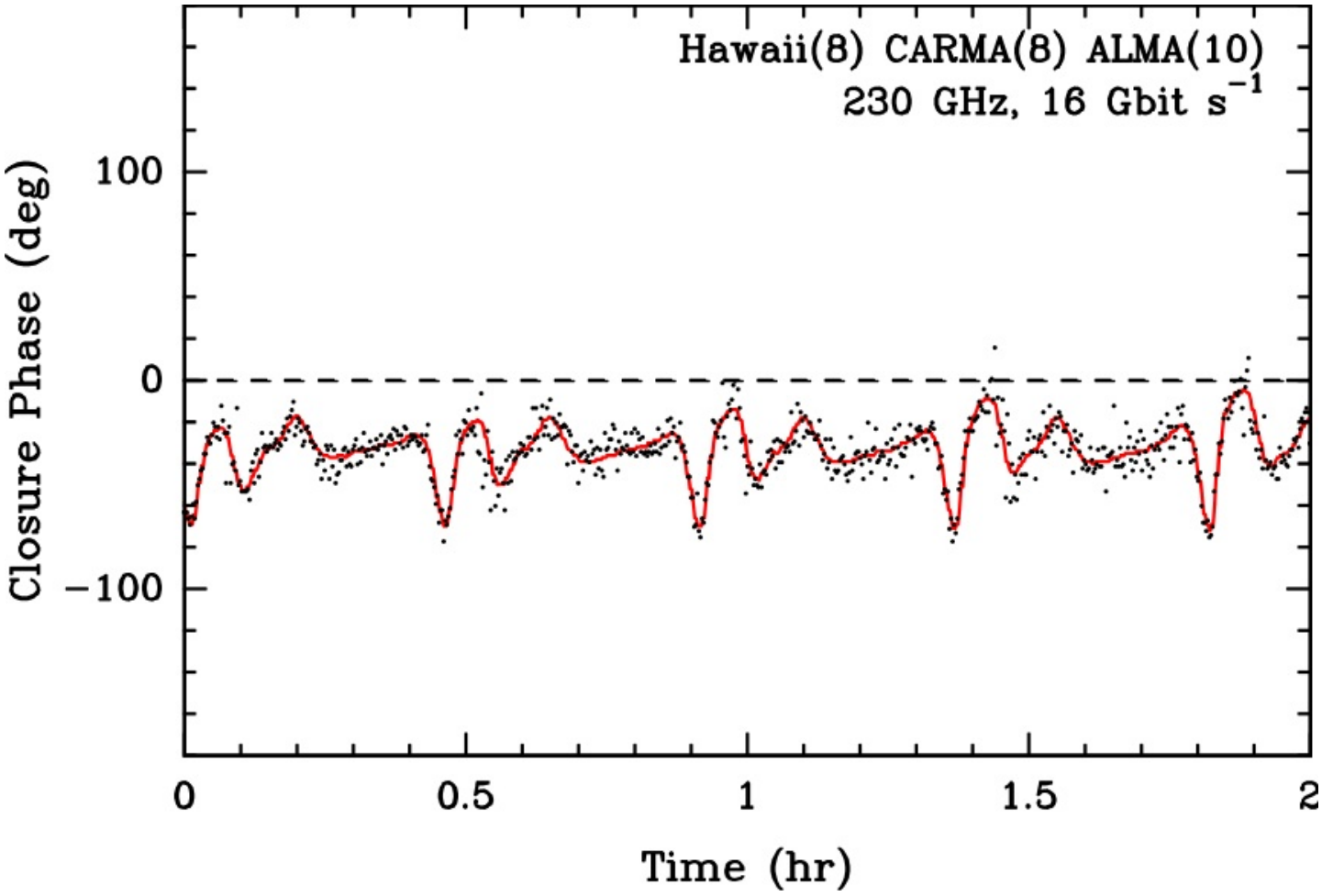

Figure 37: Closure Phase with ALMA10

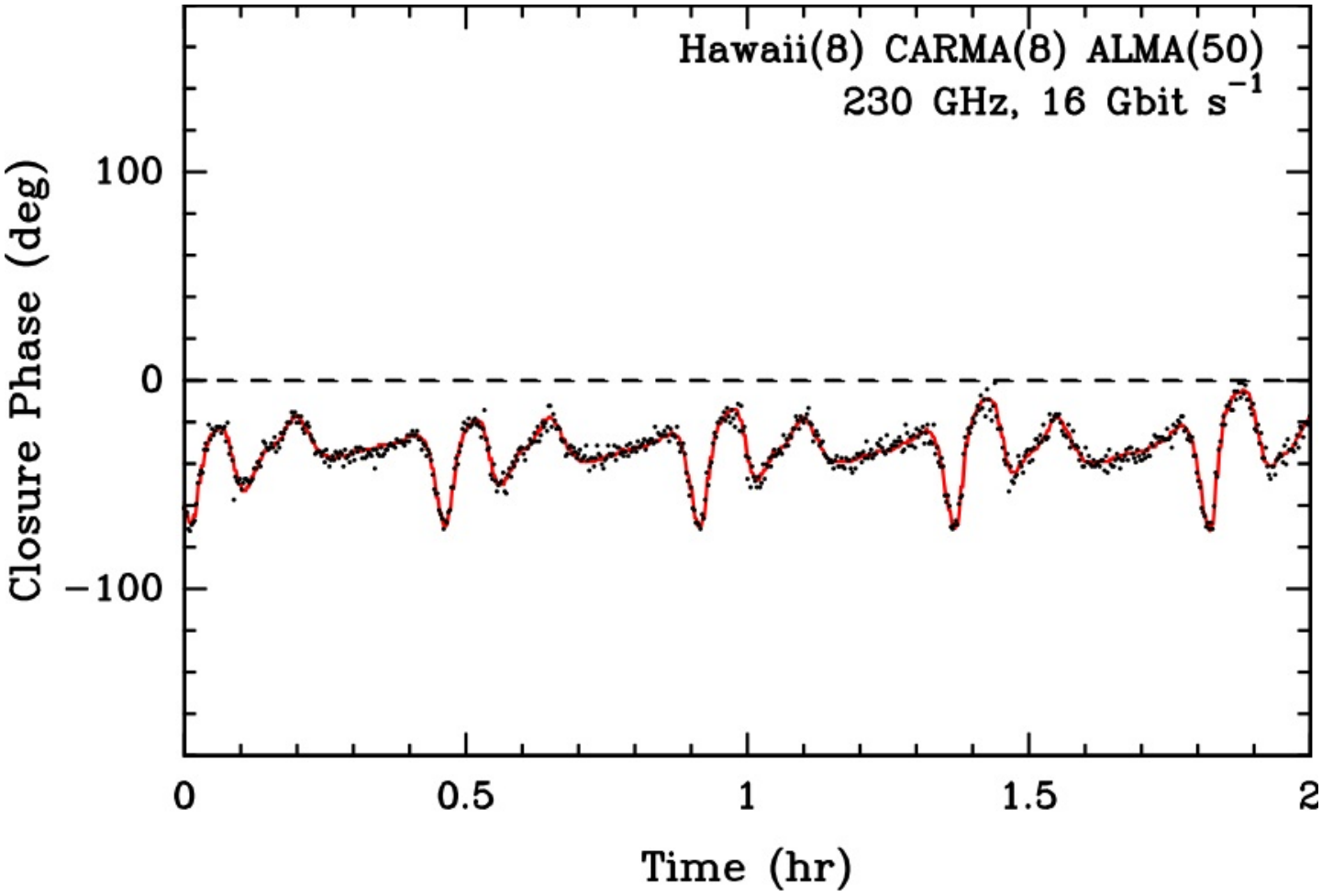

Figure 38: Closure Phase with ALMA50

SUMMARY

- Aperture synthesis enables us to map the sky brightness with sub-arcsec resolution using arrays of radio telescopes.
- Coherence of wavefront is proportional to Fourier transform of intensity distribution of source. (source and telescope $<<$ distance to source) (Van Cittert-Zernike theorem, Born & Wolf, 1959).
- The coherence (visibility function) is obtained from measurements of the cross correlation of signals between pairs of antennas.
- Telescope array with N antennas, provides $N(N-1)/2$ cross correlations and N auto correlations for each polarization product.
- Earth's rotation of the projected geometry of the telescope array in the direction of a celestial source provides additional samples of the source visibility function in the aperture plane (Ryle, 1962).

Acknowledgements

I thank the many colleagues and students who have contributed to this work, in particular the students at CASPER and summer schools at BIMA and CARMA since 1989.